

# Suppression of metal artefacts in CT using virtual sinograms and corresponding MR images

Andras Anderla<sup>1</sup>, Srdjan Sladojevic<sup>1</sup>, Gaspar Delso<sup>2</sup>, Dubravko Culibrk<sup>1</sup>, Milan Mirkovic<sup>1</sup> and Darko Stefanovic<sup>1,\*</sup>

<sup>1</sup>Department for Industrial Engineering and Management, Faculty of Technical Sciences, University of Novi Sad, Trg Dositeja Obradovica 6, 21000, Novi Sad, Serbia

<sup>2</sup>GE Healthcare, 53188, Waukesha, Wisconsin, USA

**Medical imaging is invaluable when it comes to gaining insight into the human body. As is well known, medical images need to deal with artefacts. This article presents a modern procedure for metal artifact reduction in computed tomography, which relies on additional information extracted from corresponding magnetic resonance images. We conducted a simulation study so as to compare the resulting images with those corrected, using the baseline linear interpolation method. The outcome indicates that the proposed method incomparably outperforms the baseline and reduces metal artefacts, improving the quality of images, which can be later used in a clinical setting.**

**Keywords:** Computed tomography, metal artifact, magnetic resonance imaging, virtual sonogram.

COMPUTED tomography (CT) imaging systems design cross-sectional images of tissue attenuation. Although these systems provide detailed information on a patient's internal structure, they do not provide information regarding the function of the tissues, which is needed to differentiate between normal and pathologic functions<sup>1</sup>.

The late commercialization of tri-modality imaging systems that enable the acquisition of positron emission tomography (PET), magnetic resonance (MR) and CT datasets in a single course, provides advanced opportunities for using the enhancements of all three scanners. Multimodal scanner systems brought about improvements in diagnosis, staging of a disease, treatment planning and response to therapy monitoring<sup>2</sup>. Another benefit of combining these modalities is the possibility to reduce metal artefacts in CT images using corresponding MR images.

Magnetic resonance imaging (MRI) creates images based on the relaxation properties of certain elements with nonzero magnetic moment. This allows MRI systems to extract more detailed information about the

human body than is possible with X-rays. Artefacts occur in MR images in the presence of metal. However, a study conducted by Eggers *et al.*<sup>3</sup> shows that dental fillings do not reduce the quality of images from an MRI sequence. Attempts were made in order to use MR images for the creation of attenuation maps for PET images, such as the one by Martinez-Moller *et al.*<sup>4</sup>, but the problem of effectively using MRI data to enhance information gained from other modalities remains an open research question.

MR images may suffer from signal voids which are caused by the implants. The MR artefacts present around the implant can significantly differ in composition and size. This lack of information represents the limitation of the current version of the method, and this could be overcome in the future using alternative MR sequences which are capable of imaging near the metal. Carl *et al.*<sup>5</sup> studied the likeliness of blending extremely short echo time with numerous acquisitions using different resonance image combinations to image tissues adjoining metallic implants. The results showed that there is a high possibility to greatly lower common artefacts found near the metal.

Abdoli *et al.*<sup>6</sup> developed a method which also uses the concept of virtual sinograms, but the main difference when compared to the present method is the way the affected sinogram bins are replaced. Abdoli *et al.*<sup>6</sup> used the spline interpolation technique, while the present method uses corresponding MR images which give more accurate estimations of missing projections.

This article presents a novel approach to reduce metal artefacts in CT images, utilizing additional information obtained from the corresponding MR images. This approach performs corrections in the sinogram domain using the concept of virtual sinograms, and thus differs from other proposed approaches. Typically, the missing projection data are artificially generated, while the present method relies on the information gathered from a pseudo-CT image, created from the original CT image and three corresponding MR images with different contrast settings. The corrupted values are replaced with appropriate estimates derived from the pseudo-CT image.

\*For correspondence. (e-mail: darkoste@uns.ac.rs)

For the purpose of verifying the above-mentioned method, we present correction results obtained on a set of images in which different numbers and sizes of artefacts have been simulated. The results of the proposed approach are compared with images corrected using the baseline linear interpolation method. The study shows improved performance of the suggested methodology over the baseline.

The organization of this article is as follows: first we provide an overview of relevant published work. Then we discuss the methodology used in the study and the proposed approach. The results of the experimental validation are discussed, followed by conclusions.

## Background and related work

Dark and bright streaking artefacts are actuated by the metallic implants in CT images because the atomic number of the metal is extremely high. Deprivation of the projection data is due to the high deflation of low-energy X-ray photons that pass through these objects.

Besides these effects, the literature reports various physical phenomena that direct towards artefacts in CT images. To number just a few of them: partial volume effect, Compton scattering, beam hardening, noise and respiratory and cardiac motion<sup>7</sup>.

The presence of metal objects leads to further amplification of the effects of the listed phenomena. Modern medical practice usually does not support removing metal objects from the patient, although this is sometimes done, if possible.

The literature proposes various approaches concerning metal artifact reduction. The easiest method for metal artifact avoidance would be to use less attenuating materials, such as titanium<sup>8</sup>. Another possibility is to use X-ray beams with higher energy, but limited results can be achieved using this approach at the expense of subjecting the patients to a larger dose of radiation.

There are numerous techniques aimed at exterminating or reducing the effects actuated by metallic objects which have been proposed in the literature. These can be classified into implicit and explicit techniques. Implicit approach implies suppressing artefacts without applying any algorithmic mathematical techniques. Thus, their applicability is quite limited. On the other hand, explicit methods being broader, are the main focus of contemporary research. These methods include correction in the sinogram domain<sup>9–11</sup>, improvements in the image domain<sup>12</sup>, iterative reconstruction algorithms<sup>13,14</sup>, and hybrid sinogram correction<sup>15</sup>.

All of the above-mentioned approaches are limited in the same way since they only use the data provided by CT. Metal objects form regions that have missing projection data. Due to this fact, the results are highly dependent on the number and size of metal implants found in a

patient's body. Nowadays, since tri-modality systems have become available, we have a possibility to use corresponding MR data in order to reduce the number of artefacts in CT images. This area of research is still not sufficiently explored and there are few studies that present some of the pioneer results within this field<sup>16,177</sup>.

## Materials and methods

Twelve patients from an ongoing clinical study were included in the present investigation. The patients were referred clinically and underwent a scan in a PET/CT scanner, as well as volunteering for one more MR scan. Prior to the PET scan and after the injection of <sup>18</sup>F-FDG, the patients had to rest for some time. An MR scan was done during that period. The Zurich Cantonal Ethics Committee approved this study. Before the inclusion, each patient provided a signed informed consent.

The tri-modality system used includes a GE Healthcare Discovery 690 PET/CT and a Discovery 750 W MR scanner. The MR is placed in the room right next to the PET/CT scanner. The MR table was taken to the PET/CT room using a custom-made shuttle device (Innovation Design Center, Thalwil, Switzerland). The patients did not have to change their position due to this feature.

The acquisition of PET/CT was performed according to the standardized clinical protocols regarding an oncological whole-body study (helical CT scan, 120 kV, 20–100 mA with auto-mA intensity modulation, convolution kernel 'GE-Standard' (low-pass), 512 × 512 matrix, 0.98 × 0.98 × 3.27 mm<sup>3</sup>, 2 min PET stations, ~300 MBq FDG).

LAVA-Flex, a 3D fast spoiled gradient echosequence was the MR sequence that followed. During a single acquisition, this two-point Dixon approach produces four contrasts: fat, water, in-phase and out-of-phase. This kind of sequence is repeated regularly on all whole-body tri-modality patients, in order to produce T1-weighted whole-body images necessary for anatomical localization.

For the purpose of validating the appropriate alignment of various datasets, the integrated registration tool available at the GE advantage workstation was used.

Since patients did not have dental implants, a simulation study was performed to simulate different numbers and positions of dental implants. The reason why simulated dental implants are used instead of patients with dental implants is because this approach allows the usage of images without metal artefacts as a ground truth. In the simulation study, three different set-ups were used with one, two and three dental implants respectively. Dental implants were placed only on CT images without artefacts and afterwards these images were forward-projected in order to simulate the streaking artefacts. The obtained images were used as a starting point for metal artifact suppression.

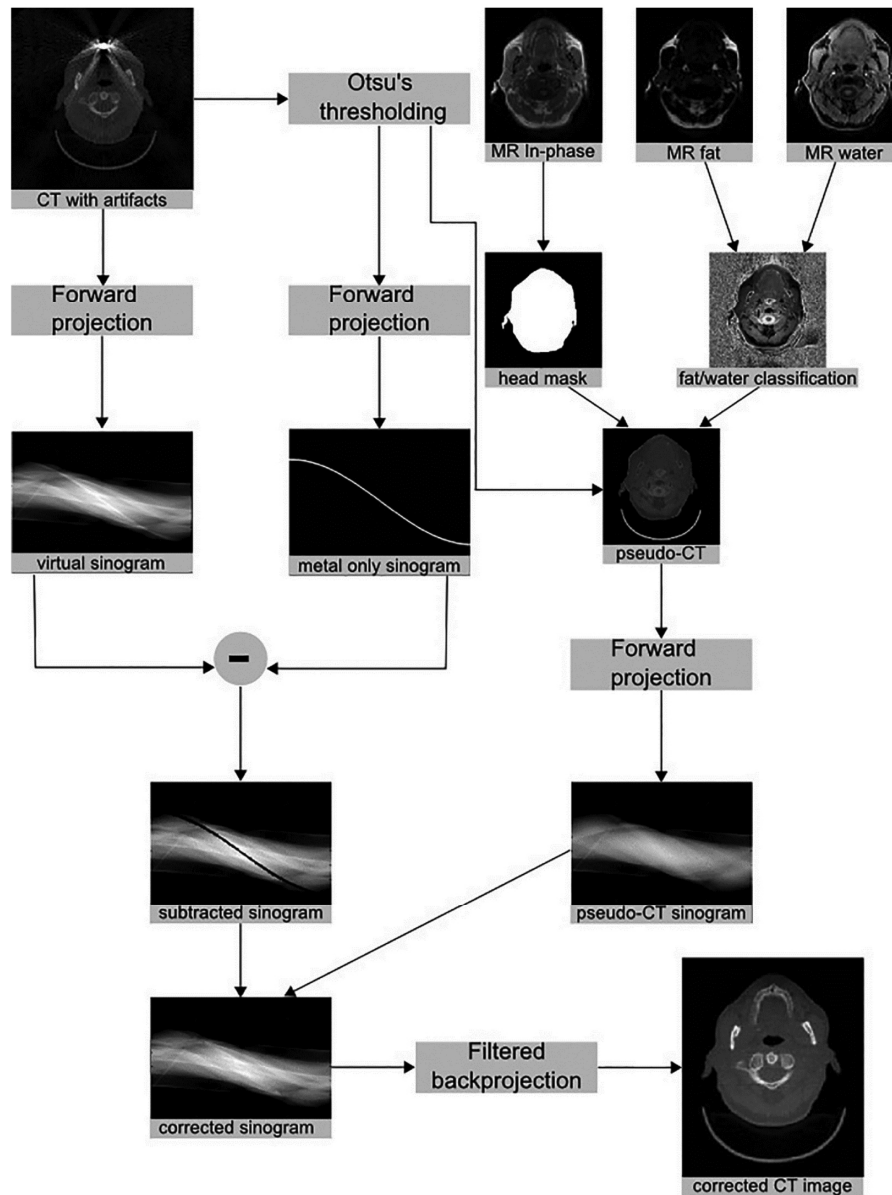


Figure 1. General overview of the suggested method.

### *Metal artifact suppression*

The suggested method consists of three main steps: detection of metal artefacts, creation of a pseudo-CT image and replacement of pixels in the metal region in virtual sinograms using appropriate estimates from the generated pseudo-CT image. Figure 1 presents a more detailed overview of the method.

### *Detection of metal artefacts*

Otsu's<sup>18</sup> thresholding method was used for the purpose of detecting artefacts in the reconstructed CT image. This approach belongs to the class of clustering-based

thresholding methods, where the grey-level data are subjected to a clustering analysis, where the number of clusters is always fixed at two. The concept of the method is as follows: first, the threshold that lowers the weighted within-class variance to a minimum has to be found. Second, the threshold has to operate directly on the grey-level histogram. The number of pixels in each class has to be balanced if the method is to produce good results.

In order to obtain the threshold, for each potential threshold:

- The pixels are separated into two clusters according to the threshold.
- The mean of each cluster is found.
- The difference between the means is squared.

- The number of pixels in one cluster is multiplied by the number in the other.

The optimal threshold is the one that lowers the within-class variance to a minimum, or, conversely, maximizes the between-class variance. The selected thresholds are less valid as the number of classes increases. The optimal number of classes for the metal region identification is 50, based on our experiments done using the images with artefacts.

Otsu's thresholding with different isolated classes is used to produce two images:

- Detected streaking lines – used for the creation of pseudo-CT image according to MR data.
- Detected origin of streaking lines – used for the creation of metal-only sinogram.

Figure 2 *b* presents the findings immediately after fixing the number of classes to  $n = 50$  and isolating those classes that do not represent artefacts. The original CT image consists of severe dental artefacts that have streaking lines (Figure 2 *a*). Upon Otsu's thresholding, the obtained mask proves the detection of the streaking lines (Figure 2 *b*).

#### *Pseudo-CT image from CT/MR data*

The pseudo-CT image is a combination of the original CT image and corresponding MR images. In the MR LAVA-Flex sequence, four contrast images were acquired: fat, water, in-phase and out-of-phase. The first three contrast images have been used in this study.

For the creation of pseudo-CT image, we used an existing approach<sup>17</sup>.

In pseudo-CT, the values outside of the skull were taken from the original CT image. The streaking lines in the background were detected with Otsu's thresholding and later left out, using only black pixel values that represent air.

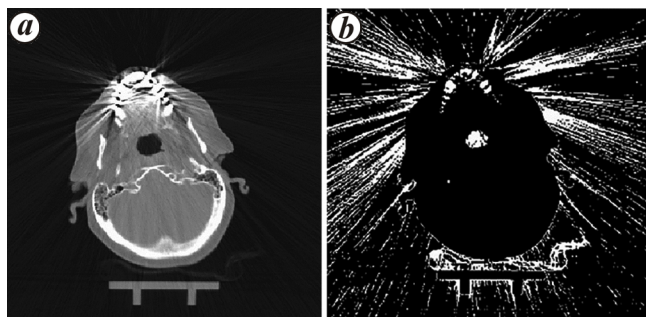


**Figure 2.** Original computed tomography (CT) image with dental streaking artefacts (*a*) and artefacts detected using Otsu's thresholding method (*b*).

In order to estimate the values inside the skull, a continuous fat/water map was created. The values for the map were calculated follows

$$CFW = -80 + 160 \frac{MRW}{MRF + MRW},$$

where CFW is the continuous fat/water map, MRF the MR image containing only fat and MRW is the MR image containing only water. The resulting image contains HU values ranging from  $-80$  HU (pure fatty tissue) to  $+80$  HU (pure soft tissue). These are the values we had set, so as to achieve corrected regions as similar to the original CT as possible. They varied slightly from the standard values used in the initial tests, where  $-84$  HU was used for fat and  $+40$  HU for muscle. Figure 3 shows the resulting continuous fat/water map.

In the next step, the MR in-phase image was used to design the head mask. This was then used to combine the continuous fat/water map and the original CT, so that the final pseudo-CT image was created.

#### *Virtual sinograms*

Virtual sinograms were created by forward projection of two-dimensional images. With this objective in mind, a projection/reprojection tool was implemented in MATLAB, similar to those proposed in the literature<sup>18,20</sup>. The projection parameters and geometry were set to duplicate the same algorithms which are used on the scanner.

CT image with simulated dental artefacts, CT image with segmented metallic objects and the pseudo-CT image were forward-projected to create their sinograms. Next, the metal-only sinogram was used to subtract it from the sinogram of the CT image with artefacts. The

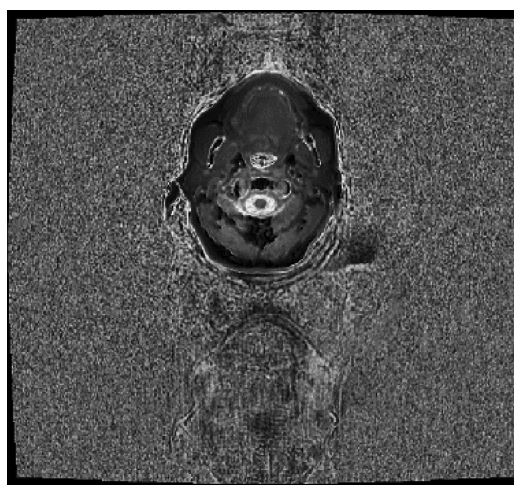


**Figure 3.** A continuous fat/water map obtained from magnetic resonance images.

resulting gap represents the missing information that has to be filled in. These missing values were first filled in with not-a-number values, so that it would be possible to easily distinguish them from the rest of the image. These values were then simply replaced with pixel values from the pseudo-CT sinogram. Finally, the corrected sinogram was backprojected using the filtered backprojection method and the artifact-free CT image was reconstructed.

For the purpose of testing the performance of the suggested approach, a simulation study was done where we made a comparison of our results to those acquired through linear interpolation. Linear interpolation represents a standard (baseline) method for missing projections reconstruction. The simulation study was carried out with the use of a cone-beam projection/reprojection tool that was also implemented in MATLAB. CT data without dental implants were used for this. Different numbers and sizes of implants were introduced and the images in the dataset were forward-projected to simulate the effects of dental implants. Sinograms were then corrected using linear interpolation and the suggested approach.

## Results and discussion

Figure 4 presents the sample findings from the simulation study. The first column contains images with simulated artefacts, while the images reconstructed with the interpolation-based method are presented in the second column. The third column presents images which are the result of the proposed approach. One should note that the performance of the linear interpolation method decreases as the number of implants increases.

Images corrected with the proposed method do not contain strong secondary artefacts, although often this can cause problems when linear interpolation is used for calculation of missing projections. Best results are achieved when the presence of metal does not have significant effect on the MR image.

It is important to provide CT images with artefacts lowered to a minimum level, since CT images are generally used with attenuation maps for making PET data correct. CT attenuation correction is much more straightforward than MR-based attenuation correction. Hence, it is possible to make an estimate of 511 keV attenuation maps from CT images. Some researchers have used MR-based attenuation correction in order to create attenuation maps from MR images in this case<sup>21,22</sup>. However, the task of discriminating the bone tissue is extremely difficult. This is a target of the present study.

A study on 152 patients in the University Hospital in Zurich showed that 122 patients (80%) had one or more dental implants and 95 patients (62%) had dental fillings that led to severe streaking artefacts<sup>17</sup>. For this purpose, our focal point was dental implants. Nonetheless, the present method does not have to be limited to only dental

fillings, but can be applied in different cases, such as hip implants and subclavian ports. The study from the University Hospital in Zurich showed that 12% of patients had subclavian ports, 5% had hip prostheses and less than 5% had some other type of orthopedic implants.

In certain cases we had incorrect registration between CT and MR images, which had as a consequence undesired occlusion of the airways. Image misregistration can occur due to hardware and patient-induced errors<sup>23</sup>. Hardware errors are related to mechanical tolerances of the shuttle system. Rigid transformations can describe and make a good approximation of hardware registration errors. On the other hand, patient-induced errors are non-rigid in nature and depend on the patient's condition, his/her comfort and anxiety. It can be noticed that these factors have more significant impact as the time between the individual scans increases. A possible solution for this is to use accurate and reproducible laser landmarking of the patient on both scanners. This method can almost eliminate received errors along the axial direction. Accurate table height adjustment can minimize misregistration along the lateral direction. Recently, Samarin *et al.*<sup>24</sup> have reported that the main offset between MR and PET/CT was below 1 cm. The Integrated Registration tool was used to further refine image registration. The registration of images was performed by the registration of MR data towards CT, taking into account the correct geometric calibration of the PET/CT system.

The approach suggested here should be tested for its practicability and robustness, for which, a greater number of patients is necessary. In addition, the size, number and position of metal objects must have some influence on the obtained results, which could be further examined.

## Conclusion

Thus in this article we have proposed a novel approach to metal artifact reduction using virtual sinograms and a dataset obtained with a tri-modality system. We have used a combination of thresholding and corresponding MR images to create the pseudo-CT image.

The method proved to be productive in exterminating streaking artefacts derived from metal implants. The proposed approach is extremely fast and fully automated. Manual interaction is not necessary, nor is it required to define the interest region.

One more asset of the proposed method lies in the fact that working on the complex raw CT data is avoidable. Currently, the application of the proposed methodology is restricted to relatively few clinical centres that contain tri-modality systems. However, the number of such institutions should increase significantly. Henceforward, the tri-modality set-up is planned to serve as a one-stop-shop for those patients who need both MR information and PET/CT during their treatment. Benefits would be

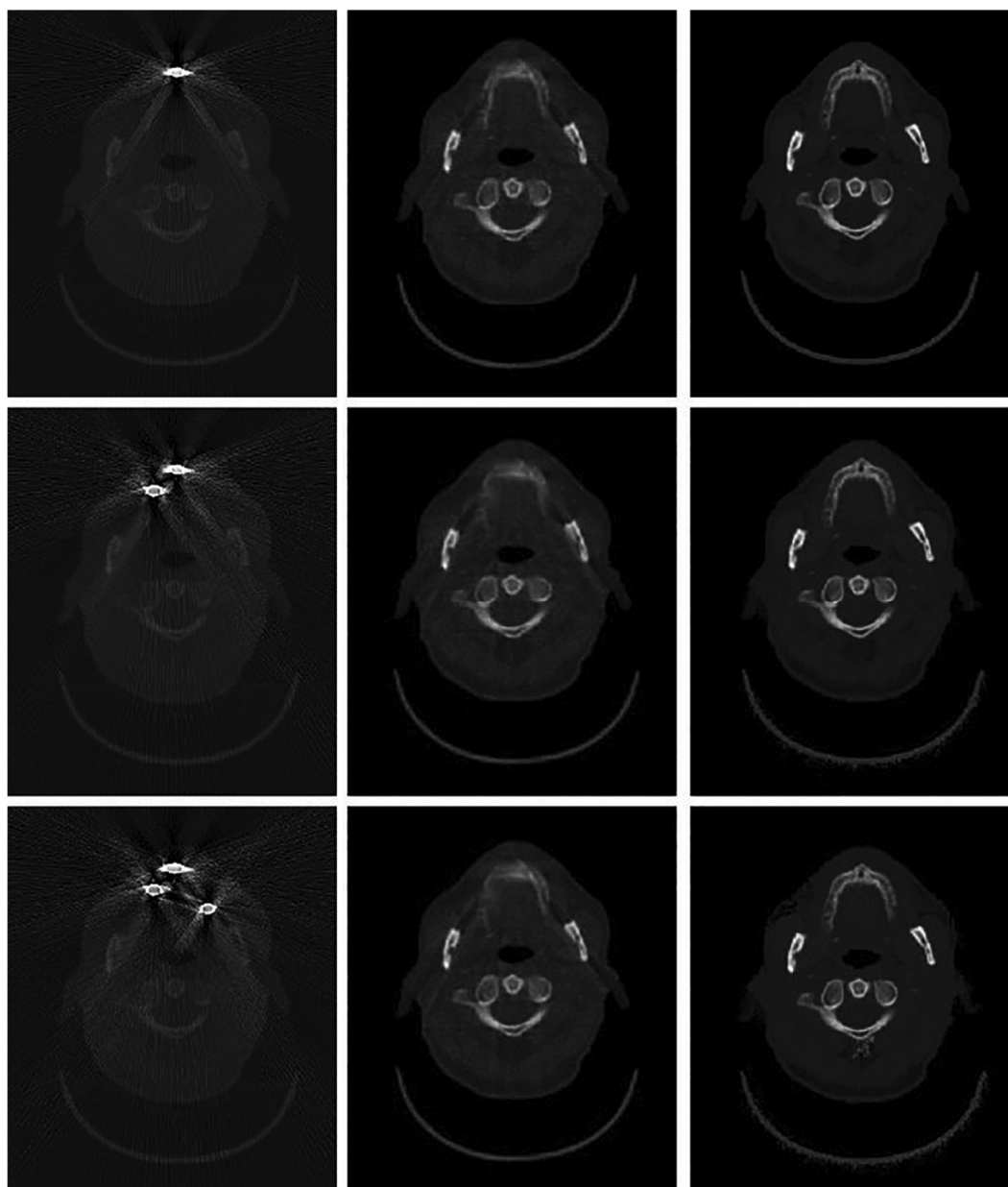


**Figure 4.** Axial view of CT dataset with simulated dental implants (left column) showing the results obtained with linear interpolation method (middle column) and the proposed method (right column).

numerous, including the possibility to spatially and temporally match datasets (clinical benefit), and to lower the costs of having separated imaging centres and patients who frequent independent imaging systems (economic benefit).

The focal point of future research will be on soft-tissue reconstruction, as well as involving a greater number of patients. In addition, the usage of raw scanner data instead of simulating them should improve the results and help this approach to be introduced into daily clinical practice.

1. Blodgett, T. M., Meltzer, C. C. and Townsend, D. W., PET/CT: form and function. *Radiology*, 2007, **242**, 360–385.

2. Townsend, D. W., Multimodality imaging of structure and function. *Phys. Med. Biol.*, 2008, **53**, R1–R39.
3. Eggers, G., Rieker, M., Kress, B., Fiebach, J., Dickhaus, H. and Hassfeld, S., Artefacts in magnetic resonance imaging caused by dental material. *Magma*, 2005, **18**, 103–111.
4. Martinez-Moller, A. *et al.*, Tissue classification as a potential approach for attenuation correction in whole-body PET/MRI: evaluation with PET/CT data. *J. Nucl. Med.*, 2009, **50**, 520–526.
5. Carl, M., Koch, K. and Du, J., MR imaging near metal with under-sampled 3D radial UTE-MAVRIC sequences. *Magn. Reson. Med.*, 2013, **69**, 27–36.
6. Abdoli, M., Ay, M. R., Ahmadian, A. and Zaidi, H., A virtual sinogram method to reduce dental metallic implant artefacts in computed tomography-based attenuation correction for PET. *Nucl. Med. Commun.*, 2010, **31**, 22–31.

7. De Man, B., Nuyts, J., Dupont, P., Marchal, G. and Suetens, P., Metal streak artifacts in X-ray computed tomography: a simulation study. In IEEE Nuclear Science Symposium and Medical Imaging Conference, 1998, vol. 3, pp. 1860–1865.
8. Klinke, T., Daboul, A., Maron, J., Gredes, T., Puls, R., Jaghsi, A. and Biffar, R., Artifacts in magnetic resonance imaging and computed tomography caused by dental implants. *PLoS ONE*, 2012, **7**, e31766.
9. Glover, G. H., An algorithm for the reduction of metal clip artifacts in CT reconstructions. *Med. Phys.*, 1981, **8**, 799.
10. Lewitt, R. M. and Bates, R. H. T., Image reconstruction from projections: III. Projection completion methods (theory). *Optik*, 1978, **50**, 189–204.
11. Hinderling, T., Ruegsegger, P., Anliker, M. and Dietschi, C., Computed tomography reconstruction from hollow projections: an application to in vivo evaluation of artificial hip joints. *J. Comp. Assist. Tomogr.*, 1979, **3**, 52–57.
12. Kennedy, J. A., Israel, O., Frenkel, A., Bar-Shalom, R. and Azhari, H., The reduction of artifacts due to metal hip implants in CT-attenuation corrected PET images from hybrid PET/CT scanners. *Med. Biol. Eng. Comput.*, 2007, **45**, 553–562.
13. Lange, K. and Carson, R., EM reconstruction algorithms for emission and transmission tomography. *J. Comput. Assist. Tomogr.*, 1984, **8**, 306–316.
14. Wang, G., Snyder, D. L., O’Sullivan, J. A. and Vannier, M. W., Iterative deblurring for CT metal artifact reduction. *IEEE Trans. Med. Imag.*, 1996, **15**, 657–664.
15. Nuyts, J. and Stroobants, S., Reduction of attenuation correction artifacts in PET-CT. *IEEE Nucl. Sci. Symp. Conf. Rec.*, 2005, **4**, 1895–1899.
16. Anderla, A., Culibrk, D., Delso, G. and Mirkovic, M., MR image based approach for metal artifact reduction in X-ray CT. *Sci. World J.*, 2013, **2013**, 1–8.
17. Delso, G., Wollenweber, S., Lonn, A., Wiesinger, F. and Veit-Haibach, P., MR-driven metal artifact reduction in PET/CT. *Phys. Med. Biol.*, 2013, **58**, 2267–2280.
18. Otsu, N., A threshold selection method from gray-level histograms. *Automatica*, 1975, **11**, 23–27.
19. Katsevich, A., A general scheme for constructing inversion algorithms for cone beam CT. *Int. J. Math. Math. Sci.*, 2003, **21**, 1305–1321.
20. Zou, Y., and Pan, X., An extended data function and its generalized backprojection for image reconstruction in helical cone-beam CT. *Phys. Med. Biol.*, 2004, **49**, N383.
21. Hofmann, M., Pichler, B., Scholkopf, B. and Beyer, T., Towards quantitative PET/MRI: a review of MR-based attenuation correction techniques. *Eur. J. Nucl. Med. Mol. Imag.*, 2009, **36**, 93–104.
22. Catana, C. *et al.*, Toward implementing an MRI-based PET attenuation-correction method for neurologic studies on the MR–PET brain prototype. *J. Nucl. Med.*, 2014, **51**, 1431–1438.
23. Veit-Haibach, P., Kuhn, F. P., Wiesinger, F., Delso, G. and von Schulthess, G., PET–MR imaging using a tri-modality PET/CT–MR system with a dedicated shuttle in clinical routine. *Magma*, 2013, **26**, 25–35.
24. Samarin, A. *et al.*, Image registration accuracy of a sequential, tri-modality PET/CT plus MR imaging setup using dedicated patient transporter systems. *Eur. J. Nucl. Med. Mol. Imag.*, 2011, **38**, S220–S220.

Received 19 January 2016; revised accepted 7 October 2016

doi: 10.18520/cs/v112/i07/1505-1511